Applied Surface Science 285P (2013) 380–388

Contents lists available at ScienceDirect

Applied Surface Science

journal homepage: www.elsevier.com/locate/apsusc

Electrochemical and morphological characterisation of polyphenazine films on copper

Carla Gouveia-Caridade, Andreia Romeiro, Christopher M.A. Brett*

Departamento de Química, Faculdade de Ciências e Tecnologia, Universidade de Coimbra, 3004-535 Coimbra, Portugal

ARTICLE INFO

Article history:
Received 7 June 2013
Received in revised form 29 July 2013
Accepted 15 August 2013
Available online 23 August 2013

Keywords:
Polyphenazine films
Morphology
Partially passivated copper
Corrosion inhibition

ABSTRACT

The morphology of films of the phenazine polymers poly(neutral red) (PNR), poly(brilliant cresyl blue) (PBCB), poly(Nile blue A) (PNB) and poly(safranine T) (PST), formed by potential cycling electropolymerisation on copper electrodes, in order to reduce the corrosion rate of copper, has been examined by scanning electron microscopy (SEM). The copper surface was initially partially passivated in sodium oxalate, hydrogen carbonate or salicylate solution, in order to inhibit copper dissolution at potentials where phenazine monomer oxidation occurs, and to induce better polymer film adhesion. SEM images were also taken of partially passivated copper in order to throw light on the different morphology and anti-corrosive behaviour of the polyphenazine films. Analysis of the morphology of the polymer-coated copper with best anti-corrosive behaviour after 72 h immersion in 0.1 M KCl, Cu/hydrogen carbonate/PNB, showed that the surface is completely covered by closely packed crystals. By contrast, images of PST films on copper partially passivated in oxalate solution, that had the least protective behaviour, showed large amounts of insoluble corrosion products after only 4 h immersion in 0.1 M KCl.

1. Introduction

Electrochemical synthesis of conducting polymers on active metal electrodes has become a subject of multidisciplinary interest in the last few years, with increased significance for corrosion protection. The electrodeposition of conducting polymers on oxidisable metals is not easy, since thermodynamic data predict that the metal will dissolve before the oxidation potential of the monomer to initiate electropolymerisation is reached. Oxidation of the metal appears as a simultaneous and competitive process to formation of the polymer. Thus, it is necessary to find electrochemical conditions which lead to partial passivation of the metal surface and decrease its dissolution rate without preventing electropolymerisation, e.g. [1].

The most investigated conducting polymers for corrosion protection of metals are polyaniline (PANI), polypyrrole (PPy) and their derivatives, e.g. [2–11]. In most of these studies PANI and PPy are electrodeposited on top of the metallic electrodes in an electrolyte solution containing the monomer, which is first used to promote formation of a passive layer and afterwards for electrodeposition of the polymer film.

Polyphenazines are very attractive redox polymers, acting both as conducting polymers and redox mediators, most of their applications being related to their use in sensors and biosensors [12]. In previous work [13,14] the phenazine monomers neutral red (NR), brilliant cresyl blue (BCB), Nile blue A (NB) and safranine T (ST) were electropolymerised on the top of copper electrodes previously passivated in oxalate, hydrogen carbonate and salicylate containing solutions. The success of the electropolymerisation depends not only on the monomer but also on the pre-passivation step, that influences the composition of the passive layer [15,16]. The anti-corrosion behaviour of the films was investigated in 0.10 M KCl using open circuit potential measurements, Tafel plots and electrochemical impedance spectroscopy. It was deduced that PNB improves the corrosion behaviour of copper electrodes, more than the other polyphenazines. PNB films on the top of copper pre-passivated in hydrogen carbonate solution had the highest protection efficiency, ~83%, calculated from Tafel plots after 4 h of immersion in 0.1 M KCl and the highest charge transfer resistance after 72 h of immersion, 27.1 kΩ cm^2 from electrochemical impedance measurements.

Since the properties of conducting polymers are strongly dependent on their morphology and structure [17], in this work scanning electron microscopy was used to examine the morphology of the polyphenazine films formed on copper electrodes. The morphology of the films with the best anti-corrosion behaviour as well as the films with the worst anti-corrosion behaviour were also analysed after 4 h and 72 h immersion in 0.1 M KCl. The mechanism of inhibition obtained from the PNB and PNR films is also discussed.

* Corresponding author. Tel.: +351 239854470; fax: +351 239827703.
E-mail address: cbrett@ci.uc.pt (C.M.A. Brett).

0169-4332/$ – see front matter © 2013 Elsevier B.V. All rights reserved.
http://dx.doi.org/10.1016/j.apsusc.2013.08.064

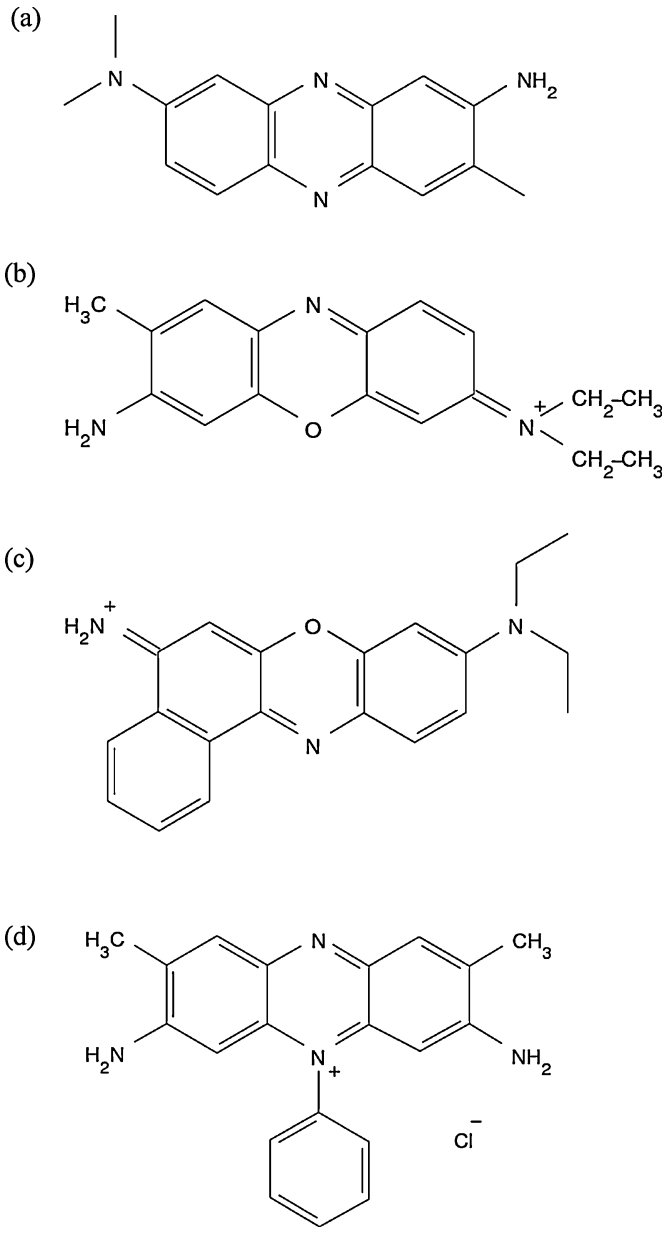

Fig. 1. Chemical structures of phenazine monomers.

2. Materials and methods

2.1. Chemicals and reagents

All chemicals were of analytical reagent grade. The electrolyte solutions used for passivation of copper were 0.125 M sodium oxalate pH 6.85 ($Na_2C_2O_4$, Merck), 0.10 M sodium hydrogen carbonate pH 8.35 ($NaHCO_3$, Riedel-de Haën, Germany), and 0.10 M sodium salicylate pH 6.50 ($NaC_7H_5O_4$, Sigma–Aldrich), concentrations optimised in previous studies. The corrosion behaviour of the modified electrodes was carried out in 0.1 M potassium chloride (KCl, Fluka).

The phenazine monomers, chemical structures shown in Fig. 1, were neutral red (NR) from Aldrich, Germany; brilliant cresyl blue (BCB) from Fluka, USA; Nile blue A (NB) from Fluka, France and Safranine T (ST) was obtained from La Chema, Czech Republic.

The correct amounts of the monomers were dissolved in the supporting electrolytes to give solutions as follows:

- 10 mM NR or 0.5 mM ST in 0.025 M potassium phosphate buffer (KPB) pH 5.54 prepared from di-potassium hydrogen phosphate trihydrate ($K_2HPO_4{\cdot}3H_2O$, Panreac, Spain) and potassium dihydrogen phosphate (KH_2PO_4, Riedel-de Haën, Germany);
- 0.5 mM BCB or 0.5 mM NB in 0.10 M sodium phosphate buffer (NaPB) pH 8.2 prepared from di-sodium hydrogen phosphate dihydrate ($Na_2HPO_4{\cdot}2H_2O$, Fluka, Germany) and sodium dihydrogen phosphate hydrate ($NaH_2PO_4{\cdot}H_2O$, Riedel-de Haën, Germany).

Millipore Milli-Q nanopure water (resistivity > 18 MΩ cm) was used for the preparation of all solutions. All experiments were performed at 24 ± 1 °C.

2.2. Instrumentation

Working electrodes were made from copper cylinders (99.99% purity, Goodfellow Metals, Cambridge, UK) by sheathing in glass and epoxy resin. The exposed disc electrode surface area was 0.20 cm^2. Before experiments, the electrodes were mechanically abraded with 400, 600, 800 and 1500 grade silicon carbide papers. After this procedure, the electrodes were rinsed with water. A platinum foil was used as counter electrode and a saturated calomel electrode (SCE) as reference in a three-electrode cell.

Cyclic voltammetry was performed using a potentiostat/galvanostat Autolab PGSTAT30 connected to a computer with general purpose electrochemical system software (GPES V4.9) from Metrohm-Autolab (Utrecht, Netherlands).

Electrochemical impedance measurements were done with a PC-controlled Solartron 1250 frequency response analyzer, coupled to a Solartron 1286 electrochemical interface using ZPlot 2.4 software (Solartron Analytical, UK). A sinusoidal voltage perturbation of amplitude 10 mV rms was applied in the frequency range between 65 kHz and 0.1 Hz with 10 frequency steps per decade.

Microscope images were acquired using a scanning electron microscope (SEM) JEOL JSM-5310 (JEOL, Tokyo, Japan), equipped with a thermionic field emission SEM and an electronically controlled automatic gun. The images were captured at 10 kV and 20 kV.

2.3. Electrode modification

Copper electrodes were partially passivated by potential cycling in sodium oxalate, salicylate or hydrogen carbonate solutions by potential cycling for 5 cycles at a scan rate of 20 mV s^{-1} in the ranges −0.5 V to +1.0 V with 0.125 M sodium oxalate, −1.0 V to +0.75 V with 0.10 M sodium hydrogen carbonate and −1.2 V to +1.5 V vs SCE with 0.10 M sodium salicylate. The passivated electrodes will be referred to as Cu/oxalate or Cu/$Na_2C_2O_4$, Cu/hydrogen carbonate or Cu/$NaHCO_3$, and Cu/salicylate.

After passivation of the copper electrodes, the phenazine films were prepared by potential scanning from solutions containing the respective monomer. The potential range depends on the electrolyte as well as on the monomer and was:

- PNR film: from −1.5 V to +1.0 V for electrodes passivated in sodium oxalate, −1.0 V to +0.25 V for electrodes passivated in sodium hydrogen carbonate and −1.2 V to +1.5 V for electrodes passivated in sodium salicylate, during 15 cycles at a scan rate of 20 mV s^{-1}.
- PBCB and PNB films: from −1.0 V to +0.5 V for electrodes passivated in sodium oxalate and −1.0 V to +0.75 V for electrodes passivated in sodium hydrogen carbonate, during 20 cycles at a scan rate of 20 mV s^{-1}.
- PST film: from −0.8 V to +0.5 V for electrodes passivated in sodium oxalate and −0.6 V to +0.3 V vs SCE for electrodes passivated in

sodium hydrogen carbonate, during 20 cycles at a scan rate of 20 mV s^{-1}.

3. Results and discussion

3.1. Effect of the electrolyte on copper passivation

Passivation of copper electrodes was done by potential cycling in sodium oxalate, hydrogen carbonate and salicylate solutions as explained in the materials and methods section. SEM images of the copper surfaces after passivation are presented in Fig. 2, as well as the first cyclic voltammograms of the copper electrode in each solution.

The passivation processes of copper in these solutions as a result of potential cycling were already discussed in detail in [12]. Briefly, in oxalate solution peak I in the cyclic voltammogram corresponds to the dissolution of copper producing Cu^{2+} ions in the vicinity of the electrode, which can interact with oxalate ions in solution, forming an insoluble copper oxalate layer on the top of the copper electrode. The electrochemical behaviour of copper in this oxalate medium is highly complex [18] with the formation of Cu–Ox complexes (where Ox denotes oxalate), such as Cu(Ox) and $(Cu(Ox)_2)^{2-}$, and copper oxides formed from Cu(I) and Cu(II). The peaks in cyclic voltammogram of Fig. 2 are attributed to the successive formation of copper products (hydroxides, oxides or complexes), that stabilise the copper surface [19]. It is stated in [20] that the copper oxalate layer is probably produced according to:

$$Cu \rightarrow Cu^{2+} + 2e^{-}$$

$$Cu^{2+} + C_2O_4{}^{2-} + H_2O \rightarrow CuC_2O_4 + H_2O$$

This rough layer is observed over the entire surface of the electrode with uniformly distributed pores (Fig. 2(a)).

In hydrogen carbonate solution the three anodic peaks in the voltammogram are related to the dissolution of copper which generates Cu(I) species in the vicinity of the electrode, until peak I is reached, leading to the formation of a film containing only Cu_2O. At higher potentials a copper (II) region is encountered, leading to growth of the passive film probably through formation of a CuO–Cu carbonate complex outer layer, within the potential range of peak II and the passive region III. Partial electroreduction of the passive film occurs at potentials corresponding to peaks IV and VI, also observed in the reduction processes of copper in NaOH solutions [21], although a passivating layer is still present on the electrode surface at −0.50 V [22].

In sodium salicylate solution (Fig. 1c), the first anodic peak at −0.17 V leads to Cu(I) and to the formation of Cu_2O while the peak at +0.20 V is related to the oxidation of copper and Cu_2O to divalent copper species on the surface and solution nearby. These Cu(II) species react with salicylate anions, adsorbing onto the electrode surface which is already modified with a Cu_2O layer and promoting the formation of a chelate [12,23–25]. The wave at ∼+0.90 V is due to salicylate ion oxidation.

After passivation in hydrogen carbonate and salicylate, the surfaces show more scratches from polishing (Fig. 2(b) and (c)), than after passivation in oxalate (Fig. 2(a)), suggesting a thicker film in the last case. This can be linked to two factors:

- the amount of formation of copper oxides and/or copper hydroxide layers and of insoluble CuO–carbonate or Cu(II) salicylate complexes on the electrode surface, in the case of hydrogen carbonate or salicylate passivating solutions, is less than of a thicker, mainly copper oxalate layer in the case of oxalate solution [12,18,20,22,23,26–28].
- differences in the initial dissolution rate of copper. As can be seen from the voltammograms in Fig. 2, the anodic current is much higher in oxalate solution, which could contribute to removing the scratches in the morphologies of the passive films, an electropolishing effect.

3.2. Effect of the passivation electrolyte on electropolymerisation of phenazine monomers

3.2.1. Electropolymerisation on Cu/oxalate passivated electrode

The phenazines neutral red (NR), brilliant cresyl blue (BCB), Nile blue (NB) and safranine T (ST) were electropolymerised on the copper electrodes passivated in oxalate solution. Representative SEM images are presented in Fig. 3, as well as cyclic voltammograms obtained during electropolymerisation of the monomers on Cu/oxalate electrodes.

The surface is completely covered by the phenazine films, PNR and PST giving granular films, the PST film having zones with a considerable number of agglomerates, and a smoother surface with pores in the case of PBCB and PNB films. Porosities calculated from Tafel plots are in agreement with what is observed from SEM images, lower for PBCB (0.01%) and higher for PNB (0.05%) [14].

The differences in film morphology can be attributed to different electropolymerisation conditions, such as the potential limits used for the potential cycling in solutions of the particular monomer and also to the electrolyte solution composition and pH. It can be seen from the voltammograms in Fig. 3 that irreversible monomer oxidation, which initiates polymerisation, occurs at positive potentials of ∼+ 0.7 V for NR, ∼+0.5 V for both BCB and NB, and ∼+0.4 V for ST.

The redox couple I/III refers to oxidation/reduction of the polymer, increasing with increasing number of cycles for all monomers tested, except in the case of NB. The increase in height of the redox couple I/III confirms polymer deposition. In the case of NB, a different behaviour was obtained in which a decrease in peak currents is observed and can be attributed to formation of a thicker and more compact semi-conductor film, which makes electron transfer more difficult [29].

3.2.2. Electropolymerisation on Cu/hydrogen carbonate passivated electrode

SEM images of the films of PNR, PBCB, PNB and PST on Cu/hydrogen carbonate electrodes are presented in Fig. 4. Cyclic voltammograms obtained during the electropolymerisation of the monomers on Cu/hydrogen carbonate electrodes are also shown in Fig. 4.

On these electrodes the films formed had different morphologies from those on Cu/oxalate electrode substrates, with many scratches observed in PBCB and PST films. As already seen in the SEM images in Fig. 2, the surface of copper passivated in hydrogen carbonate solution shows a different morphology, and it seems that this solution was less “aggressive” with less dissolution of copper metal than in oxalate solution. The adhesion of PBCB and PST films is relatively poor that also leads to a worse corrosion protection performance [14]. Nevertheless, there was evidence in the cyclic voltammograms of PBCB and PST of film formation on the top of copper. In the case of PBCB, the increase in peak currents due to polymer oxidation/reduction (peaks I and II) until cycle number 5, confirms the electropolymerisation of BCB. In cyclic voltammograms of PST the increase in peak II with a small shift to more negative potentials confirms PST formation. The shift in peak potential is due to polymer film formation and/or counterion diffusion limitations, as already observed during PNR film formation on passivated copper electrodes [13].

The SEM image of PNR on Cu/hydrogen carbonate reveals that PNR by itself forms separate agglomerates, already observed in PNR films deposited on ITO (indium-tin oxide) surfaces [30], the shape

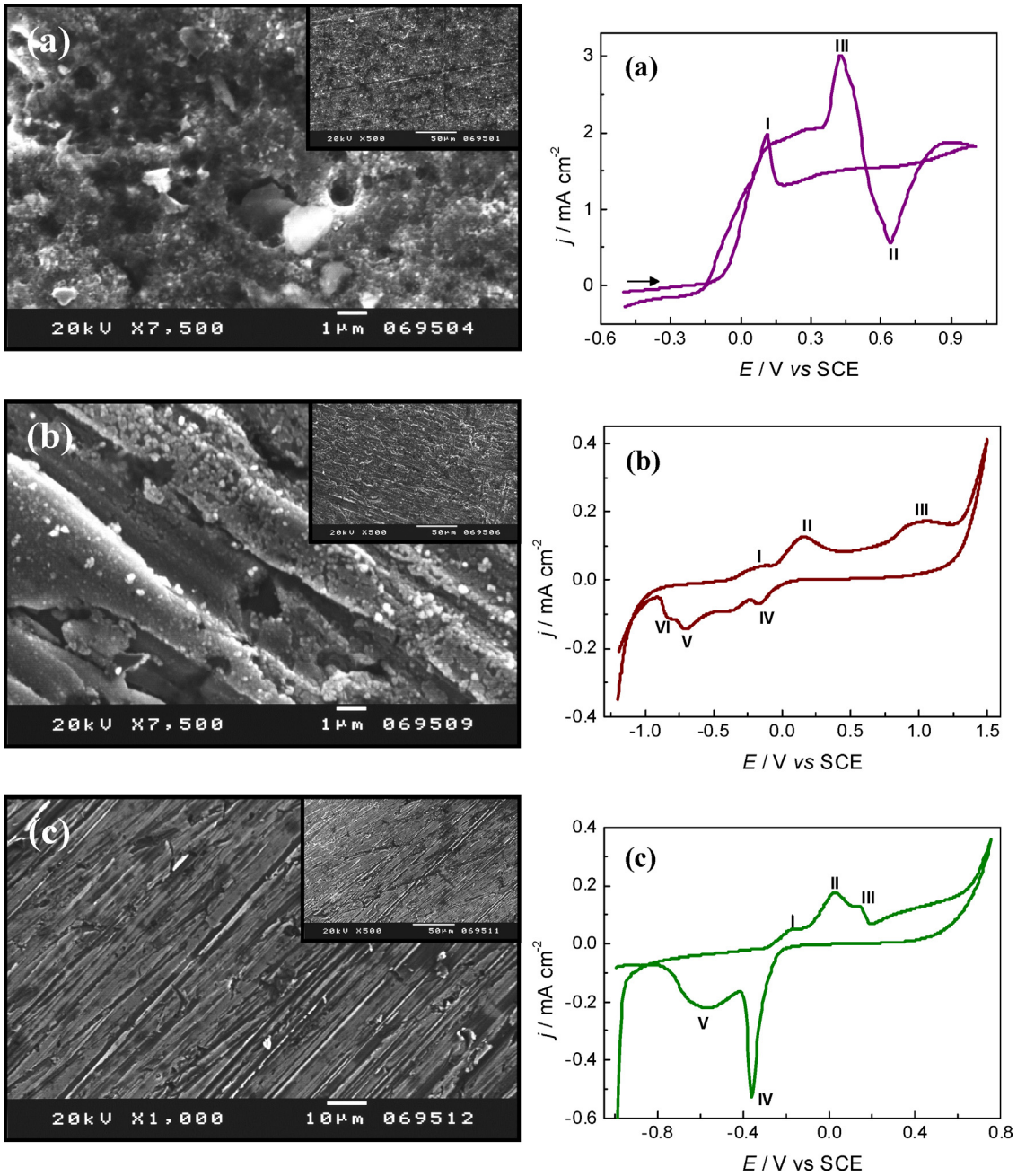

Fig. 2. Representative SEM images of films obtained after passivation of copper electrodes in sodium (a) oxalate, (b) hydrogen carbonate and (c) salicylate solutions and their respective first cyclic voltammograms.

of the voltammograms being quite similar to that obtained for PNR formation on glassy carbon [30].

The image of PNB on Cu/hydrogen carbonate (Fig. 4c) shows a compact and dense film similar to that obtained with the PNB film on Cu/oxalate electrode substrates. Some non-conductive particles observed are probably oxide formed during copper passivation. A large number of pores, of diameter ~500 nm, distributed over the whole the surface is seen, smaller than those after PNB formation of ~1 μm (Fig. 3). Again, the porosity calculated from Tafel plots [14] of 0.29% for Cu/hydrogen carbonate/PNB is in agreement with what is observed in SEM images.

3.2.3. *Electropolymerisation of PNR on Cu/salicylate passivated electrodes*

In [13], NR monomer was also electropolymerised on copper passivated in salicylate solution, but due to the slow rate of electropolymerisation and adhesion of the PNR film on Cu/salicylate as well as the lowest corrosion protection obtained, the other monomers were not studied. SEM images for PNR-coated copper are shown in Fig. 5 together with the respective cyclic voltammograms obtained during the electropolymerisation. The SEM image reveals an open structure which explains the relative lack of corrosion protection.

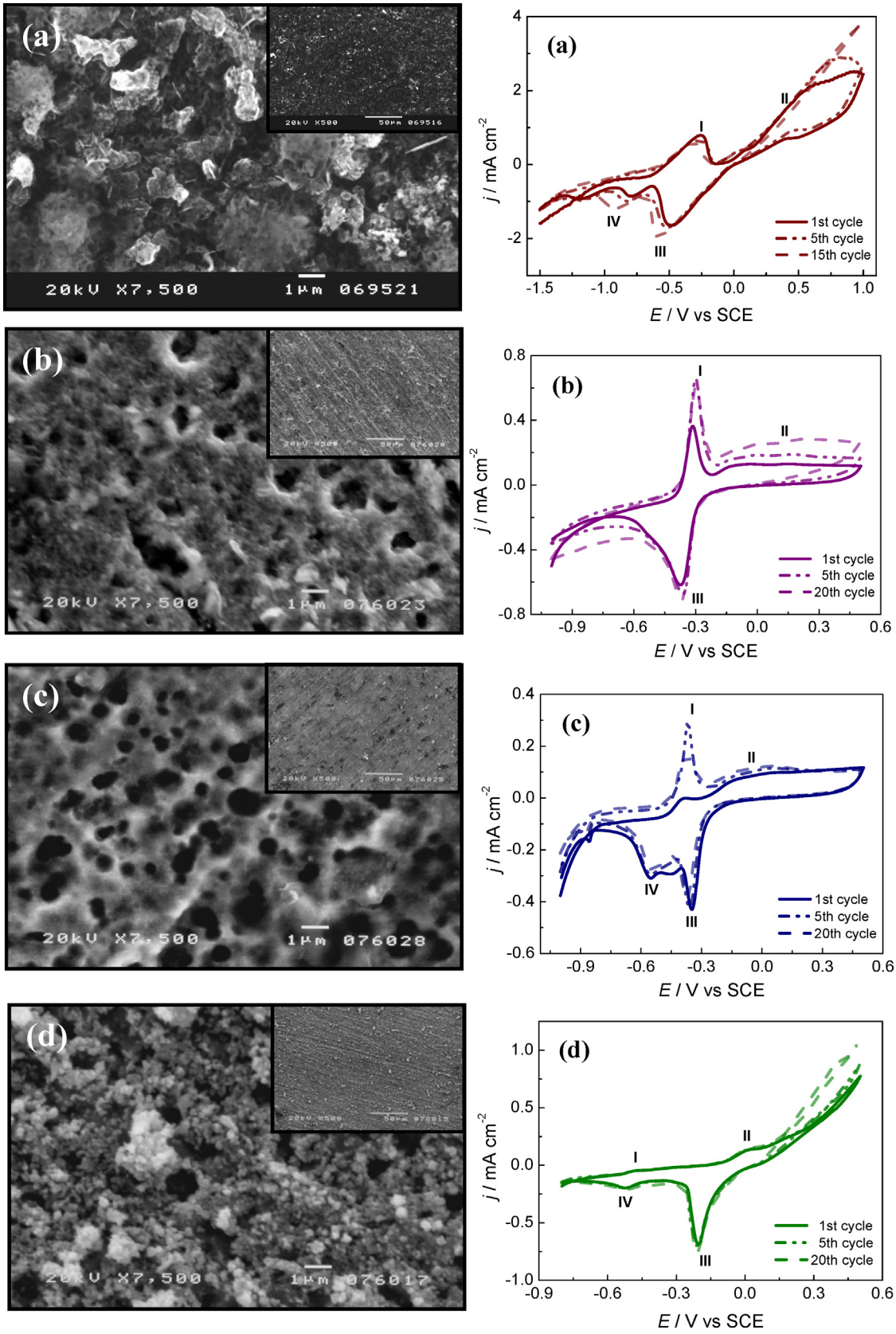

Fig. 3. Representative SEM images of films obtained from electropolymerisation of (a) NR, (b) BCB, (c) NB and (d) ST on Cu/oxalate electrode, and their respective cyclic voltammograms during electropolymerisation.

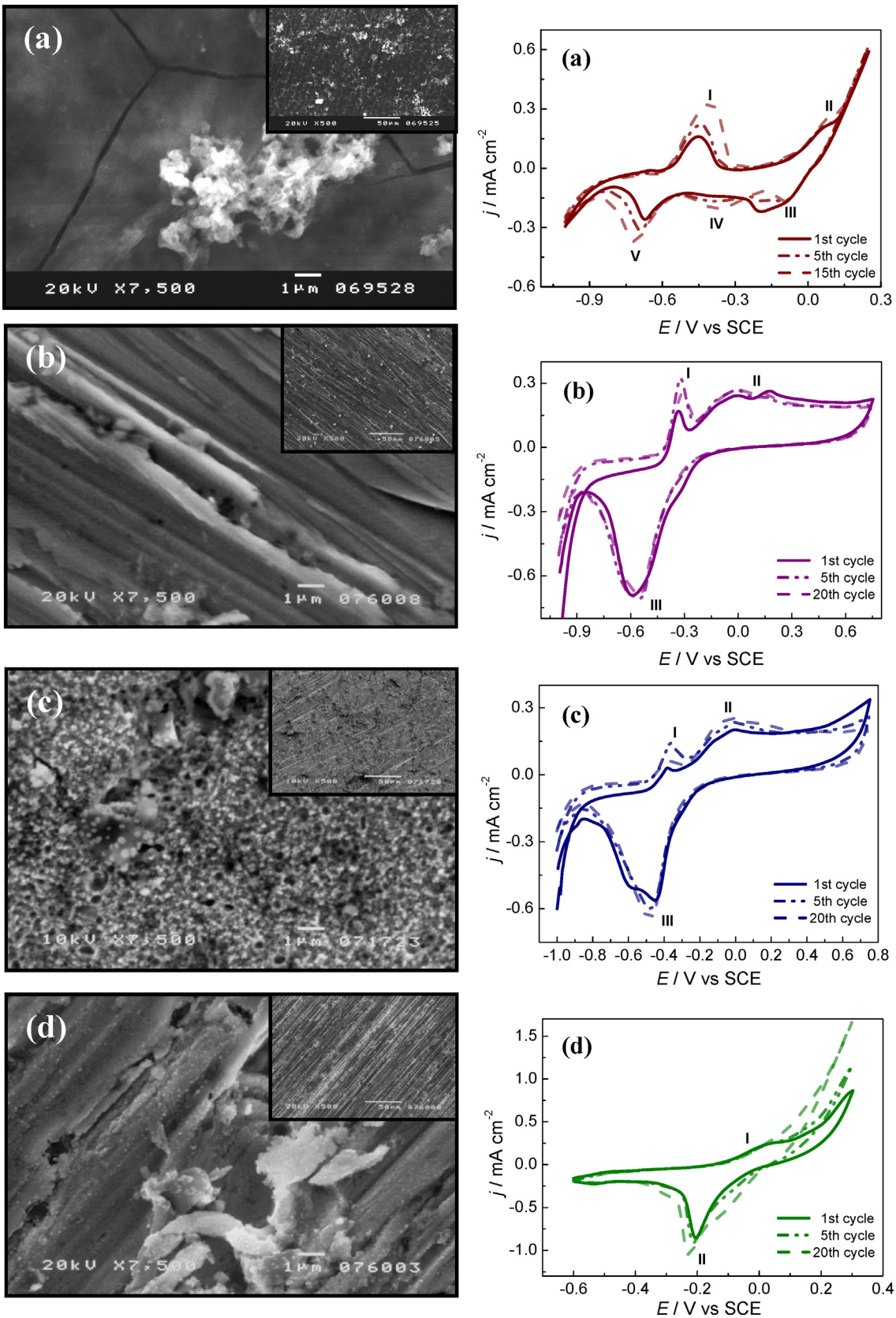

Fig. 4. Representative SEM images of films obtained from electropolymerisation of (a) NR, (b) BCB, (c) NB and (d) ST on Cu/hydrogen carbonate electrode, and their respective cyclic voltammograms during electropolymerisation.

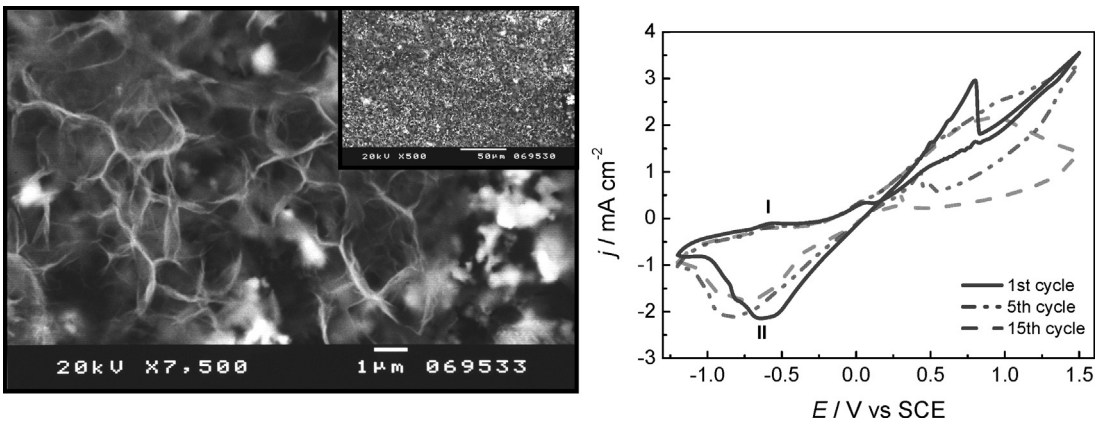

Fig. 5. Representative SEM images of the films obtained from electropolymerisation of NR on Cu/salicylate electrode, and their respective cyclic voltammograms during electropolymerisation.

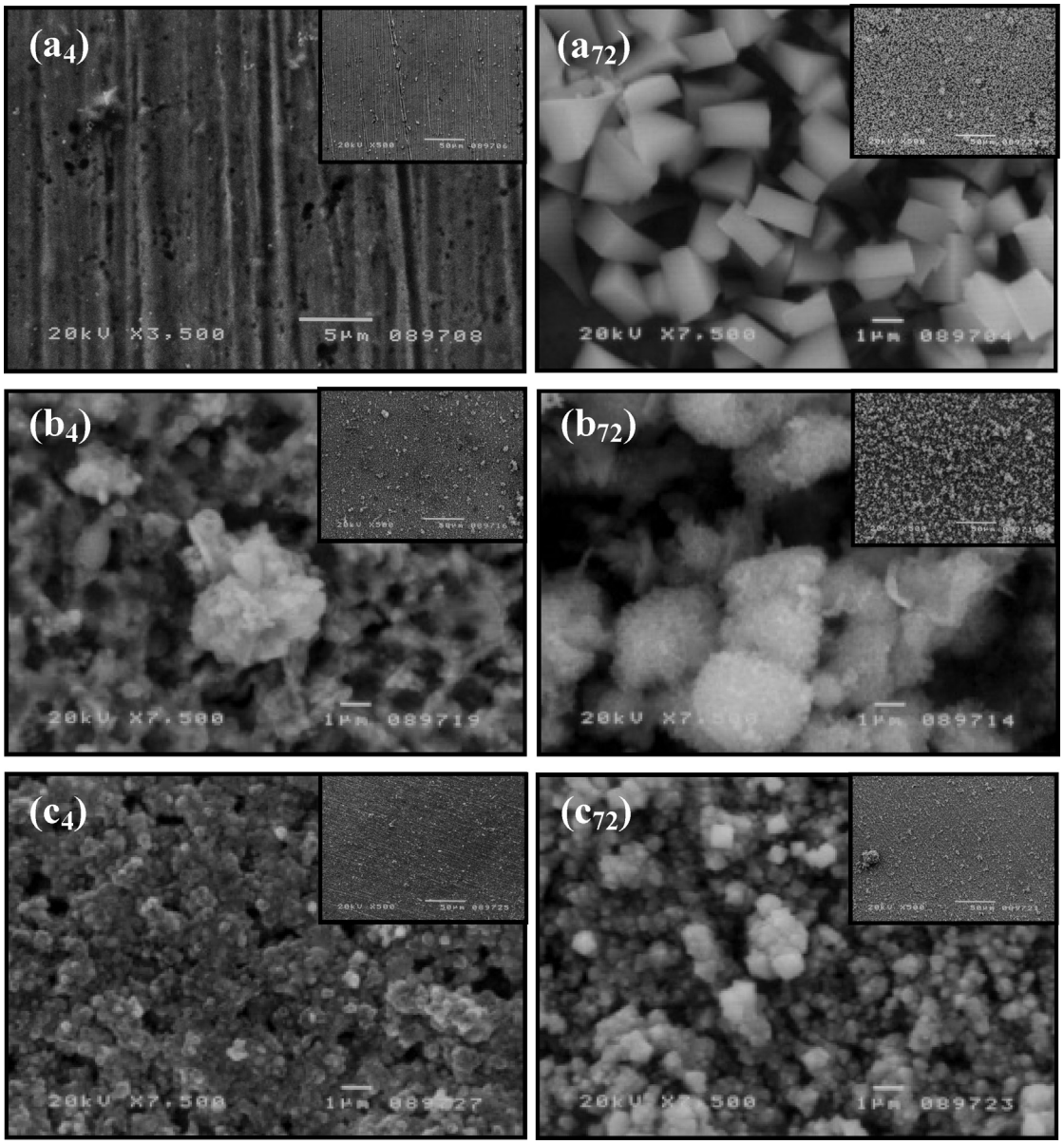

Fig. 6. Representative SEM images of (a) Cu/hydrogen carbonate/PNB, (b) Cu/oxalate/PNR and (c) Cu/oxalate/PST after immersion in 0.1 M KCl for 4 h (left side images) and 72 h (right side images).

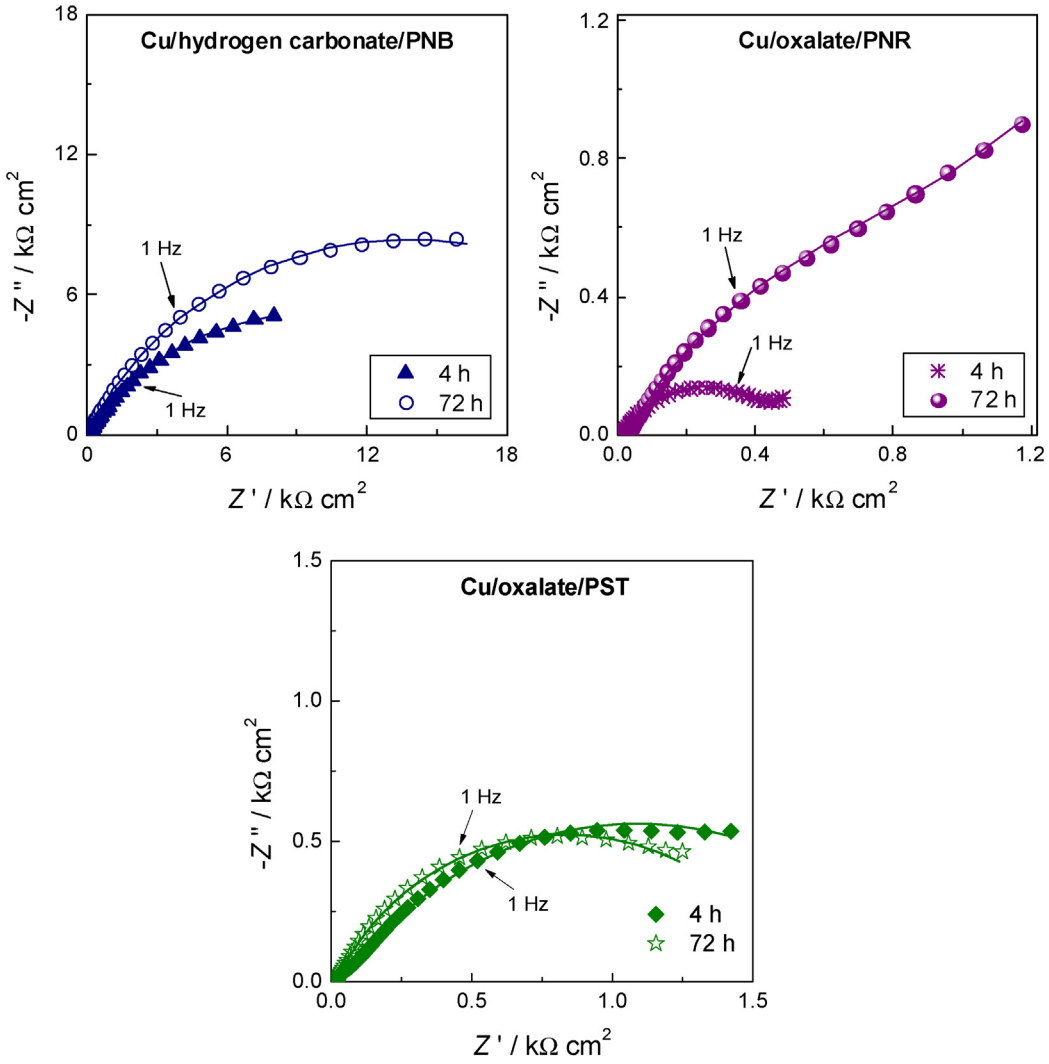

Fig. 7. Complex plane impedance spectra obtained after immersion of copper modified electrodes in 0.1 M KCl.

3.3. Polymer film-coated copper after immersion in 0.1 M KCl solution

After 4 h immersion in 0.1 M KCl, the best protection efficiency, calculated from the Tafel plots, was obtained with PNB deposited on the passivated copper electrode in sodium hydrogen carbonate solution (~83%), followed by PNR on Cu/hydrogen carbonate (~68%). A lower protection efficiency was obtained with Cu/$Na_2C_2O_4$/PST ~29%, and no protection efficiency was obtained with PBCB films [13,14]. After 72 h immersion, the highest polarisation resistances from electrochemical impedance spectroscopy were obtained with Cu/$NaHCO_3$/PNB, ~27.1 kΩ cm^2, and Cu/$Na_2C_2O_4$/PNR, ~5.9 kΩ cm^2. SEM images of selected surfaces after 4 and 72 h of immersion in 0.1 M KCl of Cu/$NaHCO_3$/PNB and Cu/$Na_2C_2O_4$/PNR and Cu/$Na_2C_2O_4$/PST are presented in Fig. 6 and complex plane impedance spectra obtained with these modified electrodes are shown in Fig. 7.

The magnitude of the impedance is higher for electrodes with PNB films, by a factor of almost 10, and increases with immersion time. The higher impedance magnitude is due to the more compact structure of the film and to the large number of pores distributed over the whole surface, see Fig. 4c, which imposes diffusion limitations on chloride ions due to their dimensions, leading to a higher film resistance and higher impedance values [14]. The increase in corrosion resistance with immersion time was also observed for copper coated with conducting polymers, e.g. [31–33], explained by the formation of a corrosion film consisted of copper chloride and/or copper oxides from diffusion of O_2 and Cl^- species from the electrolyte solution through the pores of the film. This film, with oxides filling the pores, will protect copper from further corrosion. After 4 h of immersion the PNB film (Fig. 6a) shows a large number of pores, as in Fig. 4c, and some sites with small aggregates. After 72 h of immersion the whole surface is covered by closely packed crystals. These crystals are probably corrosion products of copper oxides and chlorides in sparingly soluble atacamite ($Cu_2(OH)_3Cl$) [34–36] which fill the porous structure.

In the case of Cu/$Na_2C_2O_4$/PNR (Fig. 6b), the structure of the film after 4 h of immersion in 0.1 M KCl appears like a network, with some aggregates on the surface. After immersion for 72 h the surface is totally covered by these aggregates and has a "sponge" like appearance. The inhibition mechanism obtained with PNB and PNR films seems to be a mixture of a passivating and barrier effect. A barrier effect is predominant in earlier stages of immersion, and after the electrolyte reaches the copper surface, copper starts to corrode, leading to the formation of a film formed by corrosion products, which will be responsible for the passivating effect for longer immersion times. This film of corrosion products is well seen in SEM image of Fig. 6a_{72}.

After 4 h immersion in 0.1 M KCl, the Cu/$Na_2C_2O_4$/PST surface is covered by clusters of globules, consistent with the deposition of

large amounts of insoluble corrosion products, and the corrosion process is general dissolution of copper. This structure also appears after 72 h immersion in 0.1 M KCl.

Thus, once again there is evidence that $Cu/Na_2C_2O_4$ is the best substrate for the formation of protective PNR films and $Cu/NaHCO_3$ for the formation of PNB films.

4. Conclusions

Scanning electron microscopy has been used to investigate the morphology of phenazine films formed by electropolymerisation on pre-passivated copper electrodes in sodium oxalate, hydrogen carbonate or salicylate solutions. The copper surface was examined after passivation, and after electropolymerisation of phenazine films.

The morphology of the films depends on the passivation step solution and also on the polyphenazine. In the pre-passivation step, the use of sodium oxalate solution leads to initial intense dissolution of pure copper, and to a rough layer of Cu-oxalate that covers the entire copper surface, with a large number of pores that can be useful for increasing polymer film adhesion. In hydrogen carbonate and salicylate solutions, the initial dissolution of copper is less, and there is formation of copper oxide/hydroxide in a thin film.

On Cu/oxalate electrode substrates, the polyphenazine films cover the whole of the copper surface: PNR and PST films are granular, with some agglomerates, whereas PBCB and PNB films show a smoother, more compact structure. On Cu/hydrogen carbonate electrodes, SEM images show many scratches in the case of PBCB and PST films, PNR forms with some agglomerates, and PNB gives a smooth and compact film like that obtained with PNB on Cu/oxalate electrodes.

After 72 h immersion in 0.1 M KCl of Cu/hydrogen carbonate/PNB, the film-coated copper with the best anti-corrosion behaviour for long immersion times, the whole surface was covered by closely packed crystals of atacamite. SEM images of Cu/oxalate/PST, which had the least protective behaviour, showed general corrosion after just 4 h immersion.

The combination of morphological and electrochemical information has been demonstrated to be very useful for determination of the best redox polymers and coating strategies for the corrosion protection of copper, and extrapolation to similar coatings on other metals is envisaged.

Acknowledgements

Financial support from Fundação para a Ciência e a Tecnologia (FCT), Portugal, PTDC/QUI/65732/2006, POCH, POFC-QREN (co-financed by FSE and European Community FEDER funds through the program COMPETE and FCT project PEst-C/EME/UI0285/2013) is gratefully acknowledged. CGC thanks FCT for postdoctoral fellowship SFRH/BPD/46635/2008.

References

[1] S. Biallozor, A. Kupniewska, Synthetic Metals 155 (2005) 443.
[2] P. Herrasti, P. Ocón, Applied Surface Science 172 (2001) 276.
[3] D. Huerta-Vilca, S.R. Moraes, A.J. Motheo, Journal of Applied Polymer Science 90 (2003) 819.
[4] T. Tuken, Surface and Coatings Technology 200 (2006) 4713.
[5] S. Chaudhari, P.P. Patil, Electrochimica Acta 53 (2007) 927.
[6] R. Hasanov, S. Bilgic, Progress in Organic Coatings 64 (2009) 435.
[7] M.R. Mahmoudian, Y. Alias, W.J. Basirun, Materials Chemistry and Physics 124 (2010) 1022.
[8] A.C. Balaskas, I.A. Kartsonakis, G. Kordas, A.M. Cabral, P.J. Morais, Progress in Organic Coatings 71 (2011) 181.
[9] M.R. Mahmoudian, Y. Alias, W.J. Basirun, Progress in Organic Coatings 75 (2012) 301.
[10] V.P. Shinde, P.P. Patil, Journal of Solid State Electrochemistry 17 (2013) 29.
[11] B. Duran, G. Bereket, M. Duran, Progress in Organic Coatings 73 (2012) 162.
[12] R. Pauliukaite, M.E. Ghica, M.M. Barsan, C.M.A. Brett, Analytical Letters 43 (2010) 1588.
[13] A. Romeiro, C. Gouveia-Caridade, C.M.A. Brett, Corrosion Science 53 (2011) 3970.
[14] A. Romeiro, C. Gouveia-Caridade, C.M.A. Brett, Journal of Electroanalytical Chemistry 688 (2013) 282.
[15] D. Sazou, M. Kourouzidou, E. Pavlidou, Electrochimica Acta 52 (2007) 4385.
[16] A. Tsirimpisa, I. Kartsonakis, I. Danilidis, P. Liatsi, G. Kordas, Progress in Organic Coatings 67 (2010) 389.
[17] G. Nie, L. Qu, J. Xu, S. Zhang, Electrochimica Acta 53 (2008) 8351.
[18] A. Zouaoui, O. Stephan, M. Carrier, J.-C. Moutet, Journal of Electroanalytical Chemistry 474 (1999) 113.
[19] L.M. Martins dos Santos, J.C. Lacroix, K.I. Chane-Ching, A. Adenier, L.M. Abrantes, P.C. Lacaze, Journal of Electroanalytical Chemistry 587 (2006) 67.
[20] S. Patil, S.R. Sainkar, P.P. Patil, Applied Surface Science 225 (2004) 204.
[21] M.R.G. de Chialvo, J.O. Zerbino, S.L. Marchiano, A.J. Arvia, Journal of Applied Electrochemistry 16 (1986) 517–526.
[22] S. González, M. Pérez, M. Barrera, A.R.G. Elipe, R.M. Souto, Journal of Physical Chemistry B 102 (1998) 5483.
[23] A.C. Cascalheira, S. Aeiyach, J. Aubard, P.C. Lacaze, L.M. Abrantes, Russian Journal of Electrochemistry 40 (2004) 294.
[24] V. Shinde, A.B. Gaikwad, P.P. Patil, Surface and Coatings Technology 202 (2008) 2591.
[25] V. Annibaldi, A.D. Rooney, C.B. Breslin, Corrosion Science 59 (2012) 179.
[26] A.C. Cascalheira, L.M. Abrantes, Electrochimica Acta 49 (2004) 5023.
[27] V. Shinde, P.P. Patil, Materials Science and Engineering B 168 (2010) 142.
[28] M.P. Sánchez, R.M. Souto, M. Barrera, S. González, R.C. Salvarezza, A. Arvia, Electrochimica Acta 38 (1993) 703.
[29] J.M. Bauldreay, M.D. Archer, Electrochimica Acta 28 (1983) 1515.
[30] R.C. Carvalho, C. Gouveia-Caridade, C.M.A. Brett, Analytical and Bioanalytical Chemistry 398 (2010) 1675.
[31] P. Pawar, A.B. Gaikwad, P.P. Patil, Electrochimica Acta 52 (2007) 5958.
[32] M.I. Redondo, E. Sanchez de la Blanca, M.V. Garcia, M.J. Gonzalez-Tereja, Progress in Organic Coatings 65 (2009) 386.
[33] I. Cakmakci, B. Duran, M. Duran, G. Bereket, Corrosion Science 69 (2013) 252.
[34] M.I. Redondo, C.B. Breslin, Corrosion Science 49 (2007) 1765.
[35] L. Knuttson, E. Mattsson, B.E. Ramberg, British Corrosion Journal 7 (1972) 208.
[36] G. Kear, B.D. Barker, F.C. Walsh, Corrosion Science 46 (2004) 109.